Journal of Hazardous Materials 193 (2011) 95–101

Contents lists available at ScienceDirect

Journal of Hazardous Materials

journal homepage: www.elsevier.com/locate/jhazmat

The fate and transport of the SiO_2 nanoparticles in a granular activated carbon bed and their impact on the removal of VOCs

Hafiz H. Salih[a], Craig L. Patterson[b], George A. Sorial[a,*], Rajib Sinha[c], Radha Krishnan[c]

[a] Environmental Engineering Program, School of Energy, Environmental, Biological, & Medical Engineering, College of Engineering and Applied Science, University of Cincinnati, Cincinnati, OH 45221-0012, USA
[b] USEPA, 26 W. Martin Luther King Dr., Cincinnati, OH 45268, USA
[c] Shaw Environmental & Infrastructure, Inc., 5050 Section Ave., Cincinnati, OH 45212, USA

ARTICLE INFO

Article history:
Received 18 May 2011
Received in revised form 5 July 2011
Accepted 7 July 2011
Available online 18 July 2011

Keywords:
Activated carbon
Adsorption
Nanoparticles
SiO_2 NPs
Trichloroethylene (TCE)

ABSTRACT

Adsorption isotherm, adsorption kinetics and column breakthrough experiments evaluating trichloroethylene (TCE) adsorption onto granular activated carbon (GAC) were conducted in the presence and absence of silica nanoparticles (SiO_2 NPs). Zeta potentials of the SiO_2 NPs and the GAC were measured. Particle size distribution (PSD) of SiO_2 NPs dispersions was analyzed with time to evaluate the extent of aggregation. TEM analysis was conducted. The specific surface area and the pore size distribution of the virgin and the spent GAC were obtained. The fate and transport of the SiO_2 NPs in the GAC fixed bed and their impact on TCE adsorption were found to be a function of their zeta potential, concentration and PSD. The interaction of the SiO_2 NPs and the GAC is of an electrokinetic nature. A weak electrostatic attraction was observed between the SiO_2 NPs and the GAC. This attraction favors SiO_2 NPs attachment on the surface of GAC. SiO_2 NPs attachment onto GAC is manifested by a reduction in the amount of TCE adsorbed during the column breakthrough experiments suggesting a preloading pore blockage phenomenon. However, no effect of SiO_2 NPs was observed on the isotherm and the kinetic studies, this is mainly due to the fast kinetics of TCE adsorption.

© 2011 Elsevier B.V. All rights reserved.

1. Introduction

Trichloroethylene (TCE) is a volatile organic compound (VOC) commonly used as a cleaner in industry. This solvent is also used in metal finishing, electrical components, paint and ink formulation, and rubber processing wastewaters [1,2]. Owing to TCE's extensive commercial use and inappropriate waste disposal, it has become a significant environmental pollutant [3,4]. Its negative impact on the ecosystem and humans' health can be as severe as increased risk for cancer [5,6]. TCE is regulated by the U.S. Environmental Protection Agency USEPA at a maximum contaminant level (MCL) in drinking water of 5 μg/l. Granular activated carbon (GAC) has been regarded by the USEPA as the best available technology for removing VOCs [7]. However, the presence of background materials in water can highly impact VOCs adsorption by GAC [8]. Natural waters are thought to contain a considerable amount of nanomaterials (NMs) [9]. However, to date, the actual concentration of NMs in natural water cannot be accurately detected. Furthermore, NM may take a very long time to settle out of water, thus they are likely to reach GAC filtration in water treatment plants. Mass production and development of commercially available nanoparticles (NPs) has the potential to adversely impact GAC filtration. The high production and use of NPs in consumer products can potentially lead to high release of NPs into the environment and consequently to natural water [10,11]. NPs can be released into the environment in the stages of manufacture, refinement, application, and disposal [12]. Thus, NPs are emerging as a new type of contaminant in water and wastewater. The fate and transport of NPs in the environment have yet to be fully understood. Due to their relatively high surface area compared to their bulk counterparts, NPs can bind large quantities of pollutants [9]. Thus NPs could be seen as mobilizing vehicles for many toxic contaminants in soil, air and water.

Silica (SiO_2 NPs) are among the most common NPs that could find their way into the water system. SiO_2 NPs are naturally occurring in water as part of the colloidal system of clay (sized from a few nanometers to a few micrometers) [13]. Synthetic SiO_2 NPs are commonly used in constructing electrochemical biosensors [14], and as additives in different applications [15]. This includes applications such as anti-clumping-agents in common salts and as additives in ketchup to decrease the adhesiveness [16], printer

* Corresponding author. Tel.: +1 513 556 2987; fax: +1 513 556 4162.
E-mail addresses: salihhh@email.uc.edu (H.H. Salih), Patterson.Craig@epa.gov (C.L. Patterson), george.sorial@ucedu (G.A. Sorial), Rajib.Sinha@Shawgrp.com (R. Sinha), Radha.Krishnan@Shawgrp.com (R. Krishnan).

0304-3894/$ – see front matter © 2011 Elsevier B.V. All rights reserved.
doi:10.1016/j.jhazmat.2011.07.030

toners, cosmetics, drugs and varnishes [17]. SiO_2 NPs are causing a great concern in the field of water and waste water treatment. This is due to their possible health risk. Several investigations suggested that SiO_2 NPs may be harmful to humans [17–19]. Moreover, colloidal silica is notorious for ultrafiltration and reverse osmosis membranes fouling [13,20,21].

There are two scenarios for how SiO_2 NPs can impact the removal of VOCs by GAC. The first scenario is for SiO_2 NPs to reduce the amount of VOCs adsorbed. At a specific pH, ionic strength of the water, and based on the SiO_2 NPs and GAC electrical charge, SiO_2 NPs can attach to GAC surface and block adsorption sites and subsequently reduce the specific surface area and the amount of VOCs adsorbed. The other scenario could be for SiO_2 NPs to act as adsorption sites [9] and carry VOCs through the GAC filtration to the consumer if they are repelled from the GAC.

The main objective of this research is to study the fate and transport of the SiO_2 NPs in a GAC adsorber and its impact on the removal of TCE by GAC. This was achieved by obtaining (1) the key parameters of the SiO_2 NPs interaction with the GAC (specific surface area analysis, zeta potential and the SiO_2 NPs particle size distribution (PSD); (2) investigating the interaction between SiO_2 NPs and TCE in water i.e. the degree of adsorption of TCE on SiO_2 NPs; (3) studying the implications of SiO_2 NPs on equilibrium adsorption by conducting adsorption isotherms studies of TCE on powder activated carbon (PAC) in the presence and absence of SiO_2 NPs; and (4) studying the efficacy of a GAC adsorber bed in removing TCE in the presence of SiO_2 NPs by conducting GAC column breakthrough studies for TCE in the presence and absence of SiO_2 NPs.

2. Materials and methods

2.1. Water

All TCE solutions and NP suspensions used in the adsorption studies, PSD and zeta potential measurements, were prepared in Super-Q water with a resistivity greater than 18.3 megaohms-centimeter (MΩ cm) and a total organic carbon (TOC) concentration less than 1.0 ppb. Water used for isotherms and kinetic studies was autoclaved for 35 min at 121 °C. The water used was then buffered to a pH of 7.0 ± 0.1 with 0.001 M potassium dihydrogen phosphate (KH_2PO_4), and sodium hydroxide (NaOH).

2.2. Adsorbates

The TCE used in this research was obtained from Sigma–Aldrich (St. Louis, MO) at 99.9±% purity. Since TCE is not miscible in water, all TCE standards were prepared in methanol. Methanol final concentrations in all experiments were below 0.1% by volume. Based on previous studies, no co-solvent effects were observed at this level [22].

2.3. Activated carbon and SiO_2 NPs

A bituminous based GAC (Calgon Carbon Corporation, Pittsburgh, PA) Filtrasorb 400 (F-400) was used for all the adsorption studies. The carbon was sieved and the different particle sizes were separated. Particles 0.841–1.18 mm diameter were used for all column studies. The GAC was washed using Super-Q water and dried at 105 °C for 24 h and stored in a desiccator until used. PAC was used in all isotherm and kinetic studies to reduce the mass transfer effect of the adsorbate. PAC was obtained by crushing 500 g of the F-400 using a ball mill. PAC was then sieved and particles 125–150 μm diameter were used. This size fraction was washed using Super-Q water and dried at 105 °C for 24 h then stored in a desiccator until used.

SiO_2 NPs investigated in this research were obtained as a 30% dispersion in ethylene glycol from Alfa Aesar (Ward Hill, MA). The particle size of the SiO_2 NPs is 20 nm in diameter as reported by the vendor.

2.4. Analytical methods

Micromeritics TriStar 3000 Analyzer was used to obtain the specific surface area and pore-size distribution for the virgin and the used activated carbon. Microwave acid digestion using 20% by volume hydrofluoric acid (HF) followed by inductively coupled plasma (ICP) analysis was used to quantify the influent and effluent Si concentration for the column breakthrough study. Transmission electron microscopy (TEM) was used to obtain an exact image of the SiO_2. TCE was quantified using an Archon 5100 Purge & Trap Autosampler attached to a Tekmar 3000 Purge & Trap Concentrator. The purge and trap unit is interfaced to a Hewlett Packard 6890 gas chromatograph (GC) equipped with a flame ionization detector (FID). The GC was also equipped with an Agilent DB-WAX column (J&W 123-7063) with dimensions 60 m long × 320 μm diameter and 0.50 μm film thickness. The flow rate of the helium carrier gas was set at 2.5 milliliters per minute (ml/min). The detector makeup gas flow rate was set at 30.0 ml/min. The flow rates of the hydrogen and air flame gases were set at 35.0 ml/min and 400.0 ml/min, respectively. Tetrachloroethylene (PCE) was used as an internal standard at a concentration of 29 μg/l. The retention times for TCE and PCE were 11.9 min and 13.25 min, respectively. The detection limit for TCE was 15 μg/l.

2.5. SiO_2 and GAC characterization

The surface charge and the pH_{pzc} of the SiO_2 NPs were measured using a Malvern Zetasizer-Nanoseries at 25 °C following the analysis procedure reported by El Badawy et al. [23]. Several 10 mg/l SiO_2 suspensions were examined. The pH of the suspensions was adjusted to the range of 1.8–12.0. The charge and the pH_{pzc} of the PAC obtained using several suspensions in a pH range of 3–12.0. Samples were prepared following the analysis procedure reported by Fairey et al. [24].

SiO_2 PSD analysis was performed at SiO_2 NPs concentrations of 10.0 mg/l. SiO_2 NPs dispersions were placed in 250 ml clear glass bottles, which were continuously mixed in a rotary tumbler. One milliliter samples were collected every 30 min for the first 3 h and then every 10–15 h for three days. The Malvern Zetasizer-Nanoseries was used to measure SiO_2 NPs hydrodynamic diameter. It utilizes dynamic light scattering (DLS) with a measuring range of 0.6 nm to 6 μm.

2.6. Isotherm experiment

Three different SiO_2 NPs concentrations of 1.0, 5.0 and 10 mg/l were considered. Adsorption isotherm experiments of TCE were performed in the presence and absence of SiO_2 in these three concentrations. The adsorption isotherm experiments were conducted at a temperature of 23.0 ± 1.0 °C using the bottle-point technique where each bottle represents one data point. 250 ml Qorpak amber Boston bottles with teflon (TFE) lined closures were used in all isotherm experiments. All isotherm experiments were conducted using varied amounts of PAC (1–48 mg) and initial target concentrations of TCE of 450 μg/l; 900 μg/l and 1800 μg/l. Eight bottles per TCE concentration were run containing PAC. Six blank bottles were used per run. Three bottles per TCE concentration were run containing no PAC or NPs. The equilibrium average TCE concentration of these bottles was used to calculate the equilibrium solid phase TCE concentration (q_e). The other three blank bottles contained one of the SiO_2 NPs concentrations along with TCE, were run to

understand the interaction between SiO_2 and TCE i.e. the adsorption of TCE onto the surface of SiO_2 NPs at equilibrium. The isotherm bottles were filled completely leaving no headspace and were then continuously tumbled for two weeks to reach equilibrium. At equilibrium, samples from each bottle were filtered through a 0.45 μm filter, diluted, and analyzed using the GC. TCE adsorption equilibrium data was fitted by the Freundlich isotherm model:

$$q_e = K \times C_e^{1/n}$$

where q_e (μg/mg) is the amount of TCE adsorbed (per PAC mass) at equilibrium, C_e (μg/l) is the equilibrium aqueous phase TCE concentration, K (μg/mg (l/μg)$^{1/n}$) is a capacity parameter that expresses the extent of uptake corresponding to a value of C_e, and $1/n$ is a dimensionless parameter related to the site energy distribution [25].

2.7. Kinetics studies

Kinetic studies were conducted in order to observe the rate of TCE adsorption over time. Several kinetic studies were carried out in the presence and absence of 5.0 mg/l SiO_2 NPs. A total of ten bottles were prepared. Each bottle contained the initial target concentrations of TCE of 1800 μg/l and 0.015 mg of PAC in the presence and absence of SiO_2 NPs. Bottles were continuously tumbled. Sacrificial bottles were removed from the tumbler every 30 min for a period of 3 h. Three Samples were collected in the first 30 min at minute 1, 10 and 30. Another two samples were collected after 24 and 48 h. Samples taken from the sacrificed bottles were filtered, diluted, and analyzed in the GC.

2.8. Column breakthrough studies

The column studies were conducted using a TCE concentration of 2.0 mg/l in the presence and absence of 0.5, 1.0, 5.0 and 10 mg/l SiO_2 NPs. All breakthrough experiments were conducted using the following conditions: pH 7.0 ± 0.1, flow rate of 15 ml/min, 15.91 g of GAC mass, empty bed contact time of 2.67 min, the column diameter and length were 2.7 cm and 7.0 cm, respectively, and the mass transfer zone length was 1.6 cm. Two pressure vessels with a volume of 61 l were used as feed tanks. The solute was continuously mixed using a magnetic stirring bar. The solute was pumped from one tank at a time. Feed tanks were switched to fresh tank at a solute level of 10 l to avoid large drop in TCE concentrations. Fig. 1 shows the column experimental setup designed to overcome the volatilization of TCE out of solution by placing a constant Nitrogen gas (N_2) blanket. The two stainless steel pressure feed tanks were connected to a N_2 cylinder through a control valve. The control valve is switched on–off in response to a signal from a pressure gauge installed on the stainless steel vessels. This device allows for a constant N_2 pressure of 5 pound per square inch (psi) inside the feed tanks.

Four sample sets, from the influent and the effluent of the column were collected in a daily base to measure the TCE concentration. The flow rate and pH were also monitored and recorded.

Five milliliter samples were collected from the column influent and effluent over time. Accurate volumes of 7 ml nitric acid (HNO_3) and 3 ml HF were added to each sample. The new solutions were microwave digested using the EPA method 3051A [26]. The SiO_2 NPs concentrations were calculated by measuring Si concentrations in the digested samples. A major obstacle faced by the investigators was to obtain a representative sample. This is understandable because SiO_2 NPs were in dispersion, not in solution. Moreover, SiO_2 NPs dispersions were relatively at low concentrations. To overcome this hindrance, three samples were collected from the bottom, middle and the top of the exhausted GAC of all columns. These samples were dried for 24 h at 105 °C, degassed at 150 °C under N_2 atmosphere for 2 h, and analyzed to obtain specific surface area and pore-size distribution.

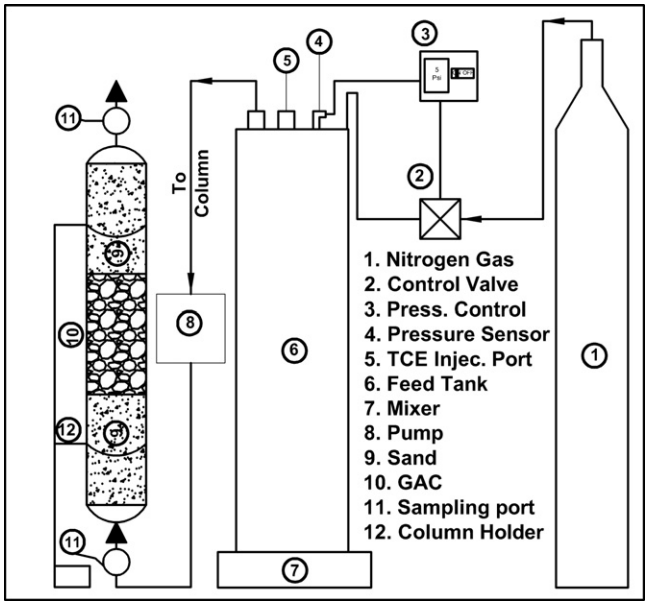

Fig. 1. Schematic diagram of the column breakthrough setup.

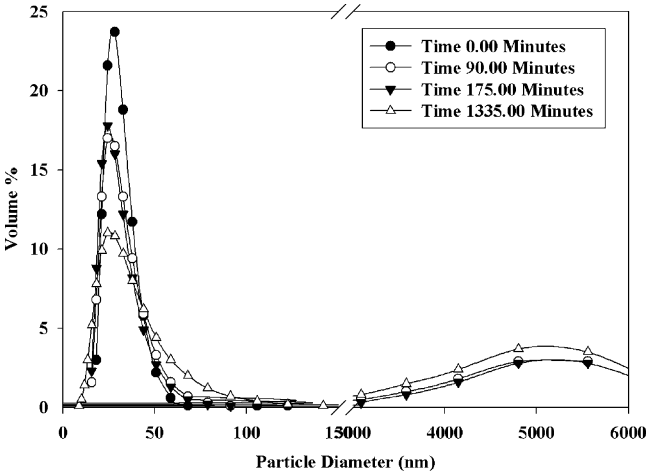

Fig. 2. SiO_2 NPs aggregation with time.

3. Results and discussion

3.1. SiO_2 and GAC characteristics

NPs have a high tendency to form aggregates, this is due to their high specific surface area to volume ratio that gives rise to vast reactivity which forces NPs to aggregate [11]. This physical phenomenon was hindered in the case of SiO_2 NPs under investigation. The SiO_2 NPs colloidal dispersion was readily dispersed in water as NPs with average diameter of 30 nm. The SiO_2 NPs PSD over a period of time is presented in Fig. 2, where the NPs diameters were plotted against the percentage of the sample volume. The data clearly suggested that the NPs dispersion is very stable. Only 10% of the particles counts have a diameter greater than 100 nm after 175 min in the rotary tumbler; which was true for three days. The stability of SiO_2 NPs is attributed to the presence of the ethylene glycol and the background electrolyte (KH_2PO_4). Ethylene glycol is a well-known

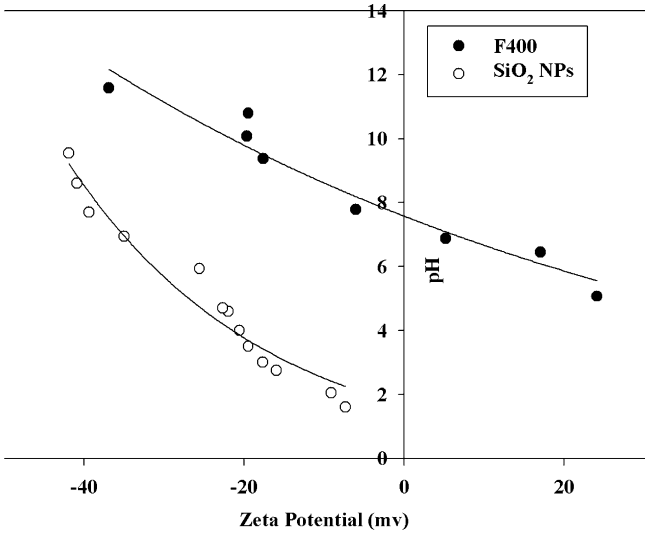

Fig. 3. GAC–SiO_2 zeta potential.

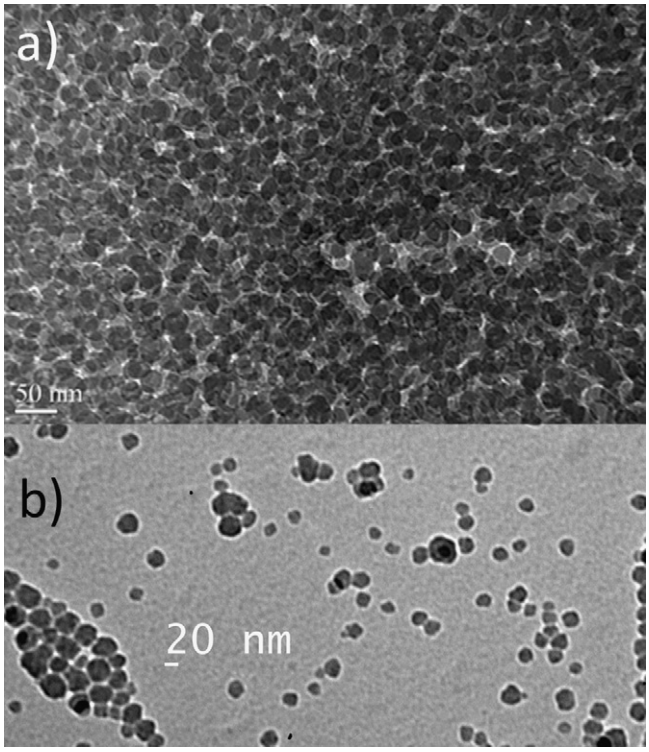

Fig. 4. (a) SiO_2 NPs as 30% dispersion in ethylene glycol. (b): SiO_2 NPs washed using methanol to remove the ethylene glycol.

capping agent. Capping agents are chemicals used to stabilize colloids by means of electrostatic repulsion, steric repulsion or both [23]. The presence of the background electrolyte has provided the diffuse electrostatic double layer (EDL) around SiO_2 NPs with a higher surface charge that generates a repulsive force between the particles and hinders the formation of aggregates [27,28]. Fig. 3 shows the surface charge and the pH_{pzc} of the SiO_2 NPs and the GAC. Evidently SiO_2 NPs have a high surface charge of −34.7 mV at pH 7.0. The other important parameter that can be deduced from Fig. 3 is the pH_{PZC}. A second order polynomial model was used to describe the zeta potential data. The EDL around SiO_2 NPs was found to be negatively charged at all pH studied with no pH_{PZC} determined. On the other hand, pH 7.6 was estimated to be the pH_{PZC} for the GAC.

Table 1
Freundlich adsorption isotherm parameters for TCE adsorption on powdered F-400 in the presence and absence SiO_2 NPs.

Isotherm Parameters	K (μg/g)/(μg/l)$^{1/n}$	$1/n$	R^2
TCE with no SiO_2	0.44	0.46	0.96
TCE + 10 mg/l SiO_2	0.39	0.49	0.99
TCE + 5 mg/l SiO_2	0.37	0.49	0.98
TCE + 1.0 mg/l SiO_2	0.39	0.50	0.98

Fig. 4(a) represents a TEM image of the 30% SiO_2 NPs dispersion in ethylene glycol. The picture is noticeably showing the uniform PSD of the SiO_2 NPs. In Fig. 4(b) the SiO_2 NPs were washed using methanol to dilute the dispersion in order to get a clearer image for separate single particle. The TEM images confirmed that SiO_2 NPs are spherical in shape. This is an important fact for SiO_2 NPs specific surface area calculation. The specific surface area of the GAC was obtained using the Micromeritics TriStar 3000 Analyzer. However, this analyzer is only capable of handling solid materials. Thus the specific surface area of SiO_2 NPs was obtained by applying a mathematical model [29].

The specific surface area (SSA) can be obtained from the equation

$$\text{SSA} = \frac{\text{Particle surface area}}{\text{Mass}} = \frac{\pi d2}{\rho(\pi/6)d3} = \frac{6}{\rho d}$$

where ρ is the density (1.3 g/cm^3) as reported by the manufacturer, d is the average particle diameter (40 nm). The SSA was determined to be 15.4 m^2/g, which is very small compared with the GAC, used in this research (745 m^2/g).

3.2. TCE adsorption isotherm

The adsorption isotherm results for TCE are presented in Fig. 5. All isotherms conducted in this study displayed a linear C_e to q_e relationship when plotted on log–log coordinates. It is further noticed that all isotherm results showed an independence from the initial aqueous phase TCE concentration (C_0). The data in Fig. 5 suggests no effect of SiO_2 NPs on TCE adsorption at equilibrium. This observation may be due to two factors. Firstly, the absence of the long range attraction which emerge in electrolyte solutions when particles (SiO_2 NPs And PAC) of opposite charge approach each other [30]. This attraction takes place when their diffusion layers approach each other. This is rational because at the working pH of 7.0 the PAC surface is almost neutral with a surface charge of −6.9 mV, while the SiO_2 NPs have −34.7 mV on its surface. This may create long range repulsion between the PAC and the SiO_2 NPs. The other reason for

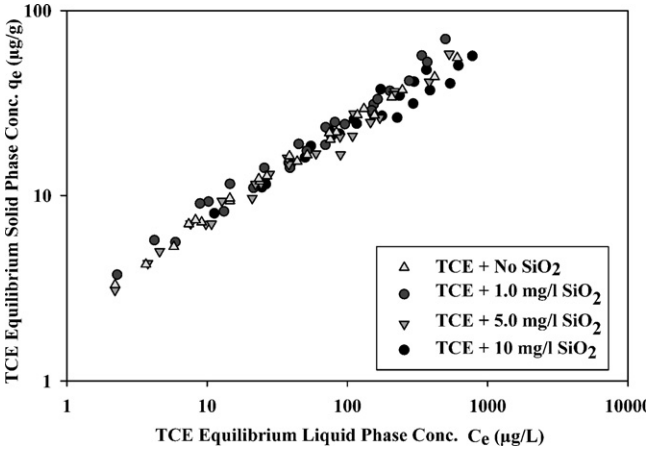

Fig. 5. Adsorption isotherms of TCE in the presence and absence of SiO_2 NPs.

Table 2
A comparison between the virgin GAC and the spent GAC from the 1.0 mg/l SiO_2 column.

Property	Virgin GAC F-400	GAC (column's bottom)	GAC (column's middle)	GAC (column's top)
BET surface area ($m^2\ g^{-1}$)[a]	745.16	600.0	625.5	617.4
Langmuir surface area (m^2/g)	1176.16	943.7	997.5	982.7
Micropore area ($m^2\ g^{-1}$)[b]	479.89	395.4	426.2	427.3
Mesopore area ($m^2\ g^{-1}$)[c]	265.27	204.7	199.3	190.1
Micropore volume ($cm^3\ g^{-1}$)[b]	0.269	0.22	0.24	0.24
Total pore volume ($cm^3\ g^{-1}$)[d]	0.484	0.39	0.41	0.40

[a] P/P° ranges from 0.03 to 0.111.
[b] t-Plot micropore area and volume.
[c] Mesopore area = BET surface area − micropore area.
[d] Single point desorption total pore volume of less than 2526.8 Å at P/P° = 0992.

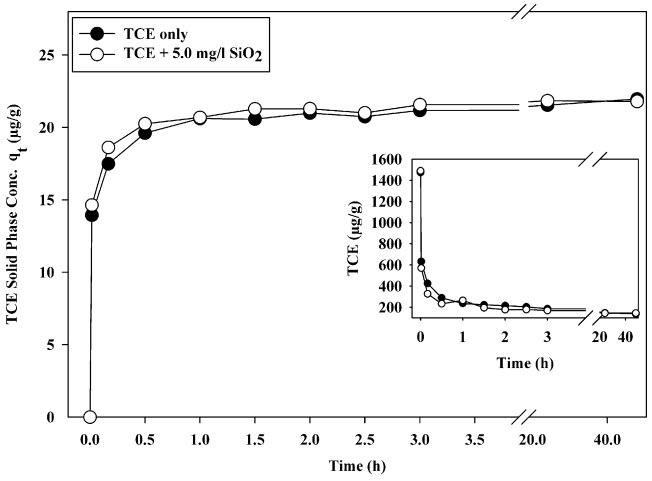

Fig. 6. TCE adsorption kinetics in the presence and absence of SiO_2.

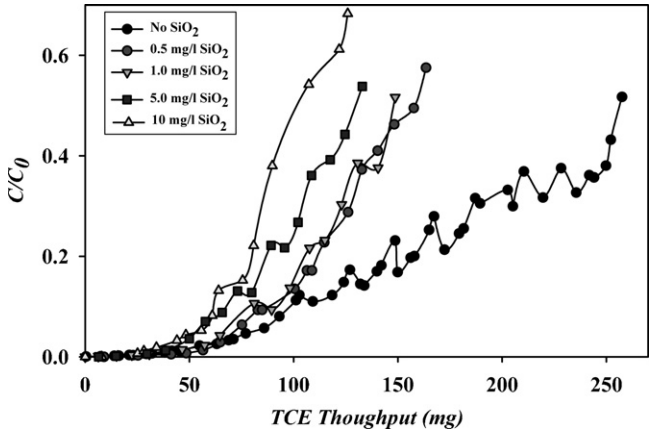

Fig. 7. TCE breakthrough in the presence and absence of SiO_2 NPs.

not seeing the SiO_2 NPs impact on TCE adsorption isotherms is the TCE adsorption kinetics. TCE has extremely fast adsorption kinetics. This fast kinetics is mainly due to the TCE molecules size and geometry. Karanfil and Dastgheib proposed that TCE has a flat profile with estimated dimensions of 0.66 nm × 0.62 nm × 0.36 nm [31]. TCE has a very small size compare to the SiO_2 NPs. This reasoning has been confirmed by the kinetics studies (Section 3.3).

The analysis of the bottles that contained TCE and SiO_2 NPs and no PAC suggested no interaction between TCE and the SiO_2 NPs (i.e. no TCE adsorbed on the SiO_2 NPs at equilibrium). The Freundlich adsorption isotherm parameters displayed in Table 1 were determined through fitting of each isotherm separately. The parameters displayed in Table 1 clearly show that there is no noteworthy difference between the four adsorption isotherms studied. In other words, there is no weighty change in Freundlich parameters between the three SiO_2 NPs concentrations used for each isotherm and in the absence of SiO_2 NPs.

An attempt has been made to investigate the possibility of TCE adsorption onto the SiO_2 NPs over a 4 h period. Several 10 mg/l SiO_2 NPs and 1.8 mg/l TCE suspensions were continuously mixed under N_2 atmosphere. Samples were collected over a period of time but filtered differently. Some samples were filtered using 0.45 μm filter while some were filtered through a 0.02 μm filter in order to remove the SiO_2 NPs and TCE if adsorption took place. The average TCE concentrations were calculated for each time period. The data obtained suggested no TCE adsorption onto the SiO_2 NPs took place during the 4 h period. It is worth noting that the blanks of TCE with SiO_2 NPs used in the isotherm study were identical with the blanks that contained no SiO_2 NPs implying no TCE adsorption onto SiO_2 NPs took place during the 15 days of equilibration.

3.3. TCE adsorption kinetics

Fig. 6 represents the TCE adsorption kinetics in the presence and absence of SiO_2 NPs. The TCE aqueous phase concentrations were measured with time. While TCE solid phase uptake at time t (q_t) calculated using the mass balance equation:

$$q_t = \frac{(C_0 - C)v}{m}$$

where C_0 is the TCE initial concentration, C is the TCE concentration at time t, v is the volume of solution and m is the PAC mass.

Results of the TCE adsorption kinetics study indicated that the majority of TCE adsorption into PAC occurs within the first 10 min. In fact 40% of the initial TCE concentration was adsorbed in the first 1.0 min. The presence of the SiO_2 NPs did not affect the TCE adsorption. This is due to the fast TCE adsorption kinetics. This also implies that the SiO_2 NPs are not competing for adsorption sites and they are limited by the film boundary layer diffusion.

3.4. Column breakthrough

Fig. 7 represents TCE breakthrough where the normalized effluent concentration to the influent concentration (C/C_0) is plotted versus TCE throughput. A 50% breakthrough ($C/C_0 = 0.5$) was set to be the breakthrough point i.e. the point at which the column experiments were stopped.

As shown in Fig. 7 the presence of the SiO_2 NPs has reduced the GAC utilization. This is manifested by rapid TCE breakthrough compared to the breakthrough conducted in the absence of SiO_2 NPs compared to the breakthrough conducted in the absence of SiO_2 NPs. The TCE rapid breakthrough is mainly due to the attachment of the SiO_2 NPs onto GAC. The NPs interaction with the GAC may have been enhanced due to the minimization of the film boundary layer in the column setting, hence, preventing external mass transfer to

be limiting factor as in the isotherm and kinetic studies. It is further seen that the impact of SiO_2 NPs on the TCE breakthrough is concentration dependent. The TCE breakthrough was the most rapid when 10 mg/l SiO_2 was present, followed by TCE breakthrough in presence of 5.0 and 1.0 mg/l SiO_2 NPs. However, this trend did not hold for the breakthrough conducted in the presence of 1.0 and 0.5 mg/l SiO_2 NPs due to the comparability of these two concentrations. These data show a capacity reduction due to the presence of SiO_2 NPs, likely due to pore blockage as supported by the pore size distribution data. This may suggest that the SiO_2 NPs behaved similarly to natural organic matter in GAC filtration [32–34].

The fate and transport of the SiO_2 NPs within the GAC column was investigated. The comparison of the spent carbon to the virgin carbon showed pore blockage and specific surface area reduction for all SiO_2 NPs concentration levels. Table 2 represents the specific surface area and the pore size distribution for the GAC samples collected from the TCE breakthrough experiment conducted in the presence of 1.0 mg/l SiO_2 NPs. The data shows reduction on the pore volume due to the pore blockage caused by the attachment of SiO_2 NPs onto the GAC surface. This attachment is expected to be on the GAC external surface i.e. the meso-pores due to the size of the SiO_2 NPs. However, meso-pores are the natural avenues to micro pores where the most of the GAC specific surface area is attributed and where TCE adsorption takes place. The largest specific surface area reduction was observed at the entrance of the column i.e. the column's bottom. The specific surface area and the pore size distribution of the other two GAC samples collected from the middle and top of the column are comparable. This is mainly due to the uniform SiO_2 NPs size distribution. The authors believe that pore blockage and reduction of GAC specific surface area are greater than the numbers listed in Table 2. This is due to the detachment of the SiO_2 NPs from the GAC external surface. During the preparation of GAC for characterization such as drying, degassing and even during sample collection after the breakthrough, SiO_2 NPs attached on the external surface of the GAC were detached.

4. Conclusions

The impact of the commercially available SiO_2 NPs on the removal of TCE by GAC was evaluated. The fate of the SiO_2 NPs within the GAC column was also appraised. SiO_2 NPs specific surface area was found to be small compared to that of the GAC. SiO_2 NPs are very stable in water due to the presence of the capping agent ethylene glycol, which hindered SiO_2 NPs from aggregating. The effect of SiO_2 NPs is a function of their zeta potential, concentration and PSD. An electrostatic interaction between SiO_2 NPs and GAC was observed at pH 7 and in the presence of 0.001 M KH_2PO_4. This interaction facilitated the attachment of SiO_2 NPs onto the GAC surface. Consequently, GAC pore blockage took place and thus the GAC specific surface area reduced. Accordingly, the presence of SiO_2 NPs decreased the amount of TCE adsorbed due to pore blockage. The interaction of TCE with SiO_2 NPs was also explored. No TCE adsorption onto the SiO_2 NPs took place over a short period of time or at equilibrium.

To validate these conclusions and to substantiate the fate of the SiO_2 NPs within the GAC Column, samples from the used GAC were collected; specific surface area and pore size distribution were obtained and compared to virgin GAC. The spent GAC showed smaller specific surface area when compared to the virgin GAC. This reduction was due to SiO_2 NPs attachment onto the GAC surface. The attachment of the SiO_2 NPs onto the GAC considerably reduced GAC's specific surface area by blocking the pores.

It is worthwhile noting that the equilibrium adsorption isotherms study showed no impact of the presence of SiO_2 NPs on the adsorption of TCE. These results indicate the weak attachment of SiO_2 and could mislead an investigator if the results will be used for mathematical model prediction of breakthrough behavior where an impact has been experimentally observed. This study clearly shows the importance of running breakthrough studies to confirm the implications of nanoparticles which is not observed in the equilibrium adsorption studies.

Acknowledgements

This work was partially supported under Contract No. EP-C-04-034 – Work Assignment No. 2-03 from the United States Environmental Protection Agency (Office of Research and Development) to Shaw Environmental & Infrastructure, Inc. and by the Cooperative Agreement of the United States Environmental Protection Agency with the University of Cincinnati under Research Traineeship Grant T-83292901-0. The finding and conclusions expressed in this publication are solely those of the authors and do not necessary reflect the views of the agency.

References

[1] S. Kim, L.B. Collins, G. Boysen, J.A. Swenberg, A. Gold, L.M. Ball, B.U. Bradford, I. Rusyn, Liquid chromatography electrospray ionization tandem mass spectrometry analysis method for simultaneous detection of trichloroacetic acid, dichloroacetic acid, S-(1,2-dichlorovinyl)glutathione and S-(1,2-dichlorovinyl)-L-cysteine , Toxicology 262 (2009) 230–238.
[2] K. Okawa, K. Suzuki, T. Takeshita, K. Nakano, Regeneration of granular activated carbon with adsorbed trichloroethylene using wet peroxide oxidation , Water Res. 41 (2007) 1045–1051.
[3] Y. Miyake, A. Sakoda, H. Yamanashi, H. Kaneda, M. Suzuki, Activated carbon adsorption of trichloroethylene (TCE) vapor stripped from TCE-contaminated water , Water Res. 37 (2003) 1852–1858.
[4] K. Wilmanski, A.N. van Breemen, Competitive adsorption of trichloroethylene and humic substances from groundwater on activated carbon , Water Res. 24 (1990) 773–779.
[5] S.L. Herren-Freund, M.A. Pereira, M.D. Khoury, G. Olson, The carcinogenicity of trichloroethylene and its metabolites, trichloroacetic acid and dichloroacetic acid, in mouse liver , Toxicol. Appl. Pharmacol. 90 (1987) 183–189.
[6] R. Crebelli, A. Carere, Genetic toxicology of 1,1,2-trichloroethylene , Mutat. Res. Rev. Mutat. Res. 221 (1989) 11–37.
[7] USEPA, The Safe Drinking Water Act (SDWA) , 1996.
[8] G.A. Sorial, S.P. Papadimas, M.T. Suidan, T.F. Speth, Competitive adsorption of vocs and bom-oxic and anoxic environments , Water Res. 28 (1994) 1907–1919.
[9] B. Pan, B. Xing, Manufactured nanoparticles and their sorption of organic chemicals , in: L.S. Donald (Ed.), Advances in Agronomy, Academic Press, 2010, pp. 137–181.
[10] S.J. Klaine, Manomaterials in the environmental: behavior, fate, bioavailability, and effects , Environ. Toxicol. 27 (2008) 1825–1851.
[11] Y. Ju-Nam, J.R. Lead, Manufactured nanoparticles: an overview of their chemistry, interactions and potential environmental implications , Sci. Total Environ. 400 (2008) 396–414.
[12] L. Reijnders, The release of TiO_2 and SiO_2 nanoparticles from nanocomposites , Polym. Degrad. Stab. 94 (2009) 873–876.
[13] X. Zhu, M. Elimelech, Colloidal fouling of reverse osmosis membranes: measurements and fouling mechanisms , Environ. Sci. Technol. 31 (1997) 3654–3662.
[14] X.-L. Luo, J.-J. Xu, W. Zhao, H.-Y. Chen, Glucose biosensor based on ENFET doped with SiO_2 nanoparticles , Sens. Actuators B 97 (2004) 249–255.
[15] L.K. Adams, D.Y. Lyon, P.J.J. Alvarez, Comparative eco-toxicity of nanoscale TiO_2, SiO_2, and ZnO water suspensions , Water Res. 40 (2006) 3527–3532.
[16] G. De, Coarsening of Ag nanoparticles in SiO_2–PEO hybrid film matrix by UV light , J. Mater. Chem. 16 (2006) 3193–3198.
[17] M. Chen, A. von Mikecz, Formation of nucleoplasmic protein aggregates impairs nuclear function in response to SiO_2 nanoparticles , Exp. Cell Res. 305 (2005) 51–62.
[18] Z. Chen, H. Meng, G. Xing, H. Yuan, F. Zhao, R. Liu, X. Chang, X. Gao, T. Wang, G. Jia, C. Ye, Z. Chai, Y. Zhao, Age-related differences in pulmonary and cardiovascular responses to SiO_2 nanoparticle inhalation: nanotoxicity has susceptible population , Environ. Sci. Technol. 42 (2008) 8985–8992.
[19] J.-S. Chang, K.L.B. Chang, D.-F. Hwang, Z.-L. Kong, In vitro cytotoxicitiy of silica nanoparticles at high concentrations strongly depends on the metabolic activity type of the cell line , Environ. Sci. Technol. 41 (2007) 2064–2068.
[20] D. Chen, L.K. Weavers, H.W. Walker, J.J. Lenhart, Ultrasonic control of ceramic membrane fouling caused by natural organic matter and silica particles , J. Membr. Sci. 276 (2006) 135–144.
[21] S. Lee, J. Cho, M. Elimelech, Combined influence of natural organic matter (NOM) and colloidal particles on nanofiltration membrane fouling , J. Membr. Sci. 262 (2005) 27–41.

[22] A. Jasper, H.H. Salih, G.A. Sorial, R. Sinha, R. Krishnan, C.L. Patterson, Impact of nanoparticles and natural organic matter on the removal of organic pollutants by activated carbon adsorption , Environ. Eng. Sci. 27 (2010) 85–93.
[23] A.M. El Badawy, T.P. Luxton, R.G. Silva, K.G. Scheckel, M.T. Suidan, T.M. Tolaymat, Impact of environmental conditions (pH, ionic strength, and electrolyte type) on the surface charge and aggregation of silver nanoparticles suspensions , Environ. Sci. Technol. 44 (2010) 1260–1266.
[24] J.L. Fairey, G.E. Speitel Jr., L.E. Katz, Impact of natural organic matter on monochloramine reduction by granular activated carbon: the role of porosity and electrostatic surface properties , Environ. Sci. Technol. 40 (2006) 4268–4273.
[25] G.A. Sorial, M.T. Suidan, R.D. Vidic, R.C. Brenner, Effect of GAC characteristics on adsorption of organic pollutants , Water Environ. Res. 65 (1993) 53–57.
[26] D.D. Link, P.J. Walter, H.M. Kingston, Development and validation of the new EPA microwave-assisted leach method 3051A , Environ. Sci. Technol. 32 (1998) 3628–3632.
[27] M. Tielemans, P. Roose, P.D. Groote, J.-C. Vanovervelt, Colloidal stability of surfactant-free radiation curable polyurethane dispersions , Coat. Sci. Int. Conf. Prog. 55 (2006) 128–136.
[28] D. Grolimund, M. Elimelech, M. Borkovec, Aggregation and deposition kinetics of mobile colloidal particles in natural porous media , Colloids Surf. A 191 (2001) 179–188.
[29] Y.P. Sun, X.Q. Li, J. Cao, W.X. Zhang, H.P. Wang, Characterization of zero-valent iron nanoparticles , Adv. Colloid Interface Sci. 120 (2006) 47–56.
[30] Y. Park, R. Huang, D.S. Corti, E.I. Franses, Colloidal dispersion stability of unilamellar DPPC vesicles in aqueous electrolyte solutions and comparisons to predictions of the DLVO theory , J. Colloid Interface Sci. 342 (2010) 300–310.
[31] T. Karanfil, S.A. Dastgheib, Trichloroethylene adsorption by fibrous and granular activated carbons: aqueous phase, gas phase, and water vapor adsorption studies , Environ. Sci. Technol. 38 (2004) 5834–5841.
[32] Q. Li, V.L. Snoeyink, B.J. Marinas, C. Campos, Pore blockage effect of NOM on atrazine adsorption kinetics of PAC: the roles of PAC pore size distribution and NOM molecular weight , Water Res. 37 (2003) 4863–4872.
[33] Q. Li, V.L. Snoeyink, C. Campos, B.J. Marinas, Displacement effect of NOM on atrazine adsorption by PACs with different pore size distributions , Environ. Sci. Technol. 36 (2002) 1510–1515.
[34] C. Pelekani, V.L. Snoeyink, Competitive adsorption in natural water: role of activated carbon pore size , Water Res. 33 (1999) 1209–1219.